

Synthesis and initial evaluation of [^{11}C](*R*)-RWAY in monkey—a new, simply labeled antagonist radioligand for imaging brain 5-HT_{1A} receptors with PET

Julie A. McCarron · Sami S. Zoghbi ·
H. Umesha Shetty · Eric S. Vermeulen ·
Håkan V. Wikström · Masanori Ichise ·
Fumihiko Yasuno · Christer Halldin · Robert B. Innis ·
Victor W. Pike

Received: 24 October 2006 / Accepted: 15 March 2007 / Published online: 20 June 2007
© Springer-Verlag 2007

Abstract

Purpose We aimed to fulfill a need for a radioligand that may be simply labeled with carbon-11 for effective positron emission tomography (PET) imaging of brain 5-HT_{1A} receptors. **Methods** Racemic RWAY (2,3,4,5,6,7-hexahydro-1-[4-[1-[4-(2-methoxyphenyl)piperazinyl]]-2-phenylbutyryl]-1*H*-azepine) has high affinity for 5-HT_{1A} receptors. The enantiomers of RWAY and *O*-desmethyl-RWAY, synthesized from commercially available materials, were each labeled with carbon-11 by treating the respective *O*-desmethyl precursor with [^{11}C]iodomethane, and injected into rhesus monkey for measurement of regional brain uptake. The 5-HT_{1A} selectivity of (*R*)-[^{11}C]RWAY was checked by administering WAY-100635, before and after radioligand administration. Radiometabolites of (*R*)-[^{11}C]RWAY in blood and urine were analyzed by HPLC with partial elucidation of their structures by LC-MS-MS.

Results (*R*)-[^{11}C]RWAY was a 5-HT_{1A} receptor antagonist exhibiting high brain uptake with regional distribution consistent with specific binding to 5-HT_{1A} receptors. The similar affinity, (*S*)-[^{11}C]RWAY was a weak partial agonist at 5-HT_{1A} receptors exhibiting similar brain peak uptake with much less 5-HT_{1A} receptor-specific binding. The maximal ratio in receptor-rich cingulate gyrus to receptor-devoid cerebellum reached 6.4 at 87.5 min after injection of (*R*)-[^{11}C]RWAY. After treatment with WAY-100635 before or after (*R*)-[^{11}C]RWAY administration, radioactivity levels in 5-HT_{1A} receptor-rich regions were reduced almost to that in cerebellum. Blood and urine radiometabolites were less lipophilic than parent and were not due to hydrolysis but to ring hydroxylations, oxidation, and dephenylation. **Conclusion** (*R*)-[^{11}C]RWAY is simply prepared and an effective antagonist for imaging brain 5-HT_{1A} receptors. This radioligand resists hydrolysis *in vivo*, gives less lipophilic radiometabolites, and warrants further PET studies in human subjects.

J. A. McCarron (✉) · S. S. Zoghbi · H. U. Shetty · M. Ichise ·
F. Yasuno · R. B. Innis · V. W. Pike
Molecular Imaging Branch, National Institute of Mental Health,
National Institutes of Health,
Building 10, B3 C346A, 10 Center Drive,
Bethesda, MD 20892, USA
e-mail: mccarroj@mail.nih.gov

E. S. Vermeulen · H. V. Wikström
Department of Medicinal Chemistry,
University Center for Pharmacy, University of Groningen,
Groningen, The Netherlands

C. Halldin
Department of Clinical Neuroscience, Psychiatry Section,
Karolinska Institutet,
Stockholm, Sweden

Keywords 5-HT_{1A} receptor · PET · Radioligand ·
[^{11}C](*R*)-RWAY · Imaging

Introduction

WAY-100635 (**1**, Fig. 1), labeled in the carbonyl position with carbon-11 (β^+ , $t_{1/2}=20.4$ min), is one of the most effective radioligands for imaging human brain 5-HT_{1A} receptors in rodent [1], monkey [2], and human subjects [3] with positron emission tomography (PET). Over the past decade, this radioligand has been used extensively for

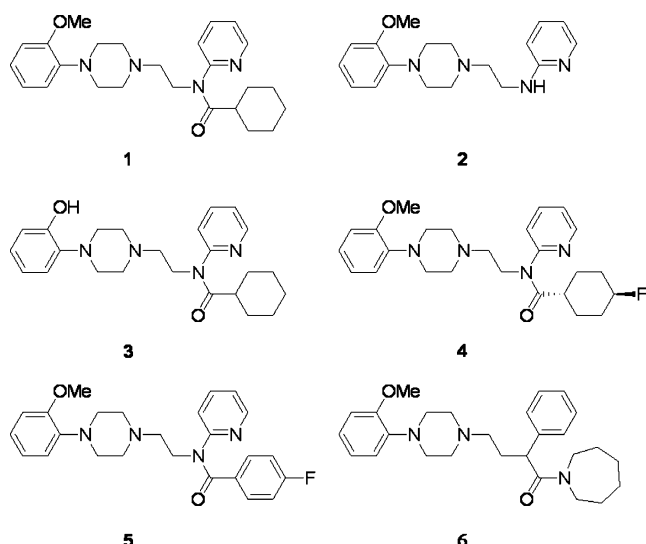


Fig. 1 Structures of 5-HT_{1A} receptor ligands and related compounds (1, WAY-100635; 2, WAY-100634; 3, *desmethyl*-WAY-100635 (DWAY); 4, FCWAY; 5, *p*-MPPF; 6, RWAY)

investigating changes in 5-HT_{1A} receptor populations in neuropsychiatric disorders and also for the development of drugs targeted at the 5-HT_{1A} receptor [4, 5]. The metabolism of **1** in monkey and humans is primarily by amide hydrolysis [6, 7]. Alternative labeling of **1** with carbon-11 in its methyl group is straightforward [1, 8] but has the drawback of giving amine **2** (WAY-100634; Fig. 1) as a brain-penetrant radiometabolite [7]. [¹¹C]**2** binds both non-specifically and specifically to brain tissue, thereby greatly reducing signal and potentially confounding PET measurements of brain 5-HT_{1A} receptors [6]. Incorporation of carbon-11 into the carbonyl moiety of **1** avoids the formation of [¹¹C]**2** and gives [¹¹C]cyclohexanecarboxylic acid as the primary radiometabolite, which gains only transient and low access to brain [7]. [*carbonyl*-¹¹C]**1** is usually prepared by treating **2** with [¹¹C]cyclohexanecarbonyl chloride [1, 9, 10], a process that has proven challenging to many PET centers. The related and superior radioligand, ¹¹C-labeled DWAY (**3**, Fig. 1), [11] is prepared similarly [1, 12]. The inherent difficulty of this type of radiosynthesis has probably hindered wider use of these radioligands. An alternative one-step radiosynthesis of [*carbonyl*-¹¹C]**1** from [¹¹C]carbon monoxide has recently been reported, but not with full details [13]. Implementation of this method may also prove challenging to many PET centers.

Two ¹⁸F-labeled radioligands for imaging human brain 5-HT_{1A} receptors are in use [4], namely ¹⁸F-labeled FCWAY (**4**, Fig. 1) [14] and *p*-MPPF (**5**, Fig. 1) [15, 16, 17]. However, these suffer from specific disadvantages. For [¹⁸F]FCWAY, extensive defluorination is problematic since this results in high skull uptake of radioactivity as [¹⁸F]fluoride ion compromising receptor measurements in nearby cortex. Such defluorination has been countered in

rats by inhibition of cytochrome P450 2E1 isozyme with miconazole [18], but this approach has not yet been established in human studies. Moreover, the radiometabolite, *trans*-4-[¹⁸F]fluoro-cyclohexanecarboxylic acid, also enters brain [19], posing further difficulty in biomathematical modeling of the acquired PET data. [¹⁸F]MPPF resists defluorination but provides a relatively much weaker signal [16, 17].

The preferred radiolabel, carbon-11 or fluorine-18, depends on the circumstances of radioligand application. Fluorine-18, because of its shorter positron range, may provide higher image resolution than carbon-11. The longer half-life of fluorine-18 allows radioligand to be transported over appreciable distances between production cyclotrons and imaging centers. Better counting statistics in brain and blood late into PET scans are also an advantage of the longer half-life. However, the longer half-life precludes multiple PET experiments in the same subject on the same day and also results in higher radiation exposure per unit of administered radioactivity. Carbon-11 has the advantage of permitting multiple PET experiments in the same subject on the same day, so avoiding many variables when comparing PET experiments performed under test and baseline conditions. Since radiation exposure per unit of administered radioactivity is generally lower, higher activities may be given to improve count statistics.

For our envisaged applications in brain 5-HT_{1A} receptor imaging, we were especially interested in using an effective ¹¹C-labeled radioligand. A new, simply labeled and effective PET radioligand for imaging animal and human brain 5-HT_{1A} receptors was considered very desirable.

Racemic RWAY [2,3,4,5,6,7-hexahydro-1-[4-[1-[4-(2-methoxyphenyl)piperazinyl]]-2-phenylbutyl]-1*H*-azepine; **6**, Fig. 1] is a known high-affinity ligand for 5-HT_{1A} receptors (IC₅₀=3 nM) [20].¹ This ligand is structurally quite similar to **1**, but the direction of its amide group is reversed. Because of this feature, **6** might be much less susceptible or completely resistant to amide hydrolysis in vivo. Moreover, each enantiomer of **6** might be simply labeled at its *O*-methyl group by treating the homochiral *O*-*desmethyl* analog (**7**) with [¹¹C]iodomethane. Hence, an enantiomer of RWAY might provide a simply labeled and effective radioligand for imaging brain 5-HT_{1A} receptors, devoid of troublesome brain-penetrant radiometabolites. Here we describe the simple radiosyntheses of [¹¹C]*(R)*-**6** and [¹¹C]*(S)*-**6** and preliminary evaluations of their radioligand behaviors in rhesus monkey with PET. [¹¹C]*(R)*-**6** is found to be a promising antagonist radioligand, while [¹¹C]*(S)*-**6** is found to be a weak partial agonist giving much lower receptor-specific signal in vivo.

¹ This patent infers that the (*S*)-(+)-enantiomer has the higher affinity for 5-HT_{1A} receptors.

Materials and methods

General

All compounds and reagents for syntheses were purchased from Aldrich, except for the following: triethylamine (TEA), lithium diisopropylamide (LDA) and bromine (Acros), 2-bromoethanol (Alfa Aesar), 2-phenyl-acetyl chloride (Fluka), 2-methoxy-piperazine (Lancaster), and potassium carbonate (Boom). Chromatographic grade solvents were purchased from Burdick & Jackson. Tetrabutylammonium hydroxide (TBAH; 1 M solution in methanol) was purchased from Aldrich and diluted to 0.167 M with methanol (Burdick & Jackson).

Chemistry

1-Azepan-1-yl-2-phenylethanone (8) 2-Phenyl-acetyl chloride (3.5 g; 25 mmol) was freshly prepared from 2-phenyl-acetic acid and thionyl chloride and then dissolved with cyclohexylimine (2.48 g; 25 mmol) in chloroform (25 ml) at 0°C under nitrogen. TEA (5.0 g; 50 mmol) was added. The reaction mixture was allowed to warm to room temperature (RT), stirred overnight, diluted with dichloromethane (150 ml), and then washed successively with hydrochloric acid (1.0 M; 20 ml), water (20 ml), and sodium bicarbonate solution (sat'd.; 20 ml). The organic layer was dried over sodium sulfate, filtered, and concentrated in vacuo to give an orange oil. This product was purified by distillation at 150°C (0.05 mBar) to give **8** as a yellow oil (4.61 g; 93%). ¹H-NMR (CDCl₃, 300 MHz) δ (ppm) 1.42–1.68 (m, 8H), 3.37 (t, *J*=5.9 Hz, 2H), 3.46–3.5 (m, 2H), 3.66 (s, 2H), 7.15–7.28 (m, 5H). IR (neat; cm⁻¹) 3456, 3029, 2927, 2855, 1734, 1632, 1453, 1275, 1151, 1030, 725, 697. GC-MS (EI+): 217, 126, 91, 55 (100%).

2-[4-(2-Methoxyphenyl)-piperaziny-1-yl]-ethanol (9) [21] 2-Methoxyphenyl-piperazine (2.0 g; 10 mmol) was dissolved in ethanol (25 ml). Potassium carbonate (3.56 g; 25 mmol) was added at RT, followed by 2-bromoethanol (1.56 g; 12.5 mmol). The reaction mixture was refluxed overnight, cooled to RT, and concentrated in vacuo. The residue was taken up in dichloromethane and washed with aqueous sodium bicarbonate. The organic phase was dried over sodium sulfate, filtered, and concentrated in vacuo to give **9** as a yellow oil (2.22 g; 94%). ¹H-NMR (CDCl₃, 300 MHz): δ (ppm) 1.62 (br, 1H), 2.57 (t, *J*=5.5 Hz, 2H), 2.66–2.69 (m, 4H), 3.05 (br, 4H), 3.59–3.62 (m, 2H), 3.81 (s, 3H), 6.8–6.96 (m, 4H). IR (neat; cm⁻¹) 3400, 2940, 2819, 1593, 1502, 1453, 1240, 1144, 1027, 943, 749. MS (EI+): 236, 205, 190, 162, 120, 91, 70 (100%).

1-(2-Bromo-ethyl)-4-(2-methoxyphenyl)piperazine hydrobromide (10) [22] Triphenyl-phosphine (3.7 g; 14.1 mmol)

and **7** (2.23 g; 9.41 mmol) were dissolved in dichloromethane under nitrogen at 0°C. Bromine (2.28 g, 14.3 mmol) was added dropwise. After 30 min, the reaction mixture was warmed to RT and stirred for 1 h. The white precipitate was filtered off and dried in vacuo to give **10** (3.50 g; 98%). ¹H-NMR (CDCl₃; 300 MHz): δ (ppm) 2.72–2.79 (m, 4H), 2.84 (d, *J*=7.33 Hz, 2H), 3.1–3.15 (m, 4H), 3.61–3.68 (m, 2H), 3.87 (s, 3H), 6.85–7.02 (m, 4H). IR (KBr; cm⁻¹): 3450, 3340, 3002, 2628, 2520, 2435, 1612, 1502, 1452, 1296, 1295, 1117, 1014, 960, 756, 634. MS (EI+) 300/298, 219 (100 %), 190, 162, 120, 84, 56.

2,3,4,5,6,7-Hexahydro-1-[4-[1-[4-(2-methoxyphenyl)piperaziny]]-2-phenylbutyryl]-1H-azepine (RWAY) (6) [20] Compound **8** (0.69 g; 3.17 mmol) was dissolved in tetrahydrofuran (THF; 20 ml) under nitrogen and cooled to 0°C. LDA (2 M in pentane; 3.25 ml) was added dropwise. After 30 min, a solution of **10** (0.95 g; 3.17 mmol) in THF (10 ml) was added slowly. The reaction mixture was then warmed to RT, stirred overnight, and quenched with water (50 ml). Volatile compounds were removed under reduced pressure. The residue was dissolved in dichloromethane and washed with saturated sodium bicarbonate solution. The organic layer was separated off, dried over sodium sulfate, filtered, and concentrated under reduced pressure. The residue was purified by flash chromatography (silica gel, CH₂Cl₂/MeOH, 98/2 with 0.1% TEA) to give **6** as a colorless oil (0.66 g; 48%). ¹H-NMR (CDCl₃, 300 MHz) δ (ppm) 1.46–1.58 (m, 5H), 1.6–1.78 (m, 3H), 1.85–2.0 (m, 1H), 2.31–2.58 (m, 3H), 2.76 (br, 4H), 3.16 (br, 4H), 3.22–3.76 (m, 4H) 3.85 (s, 3H), 3.95–4.05 (m, 1H) 6.88–6.97 (m, 4H), 7.26–7.34 (m, 5H). IR (neat cm⁻¹) 2929, 2813, 1633, 1500, 1446, 1240, 1025, 748, 701. MS (EI⁺): 435, 420, 337, 273, 244, 219 (100 %), 204, 190, 162, 126, 70.

(S)-6 and (R)-6 Compound **6** was resolved into its enantiomers by chromatography on a Chiral-Pak AD column (25×1 cm; Daicel) eluted at 4 ml/min with hexane-2-propanol-TEA (95:5:0.1 by vol.): *(S)-6* ([α]_D (CHCl₃)=+73.3°, *t*_R=5.7 min; *(R)-6* ([α]_D (CHCl₃)=-77.8°, *t*_R=7.5 min. HRMS for each enantiomer: required for [C₂₇H₃₈N₃O₂]⁺ *m/z* 436.2958; found 436.2964.

2,3,4,5,6,7-Hexahydro-1-[4-[1-[4-(2-hydroxyphenyl)piperaziny]]-2-phenylbutyryl]-1H-azepine (7) Aluminum chloride (0.92 g; 6.9 mmol) was added to **6** (0.3 g; 0.69 mmol) in benzene (25 ml) and the reaction mixture refluxed for 48 h. The cooled mixture was then poured into saturated sodium bicarbonate solution (50 ml). The organic materials were extracted into dichloromethane (3×20 ml). Extracts were combined, dried over sodium sulfate, filtered, and concentrated in vacuo to give a brown oil (0.25 g; 83%). Chromatography of this oil (silica gel, CH₂Cl₂-MeOH with 0.1% TEA) gave pure

7. $^1\text{H-NMR}$ (CDCl_3 , 300 MHz): δ (ppm) 1.21–1.34 (m, 2H), 1.44 (br, 4H), 1.62–1.68 (m, 3H), 1.8–1.88 (m, 1H), 2.27–2.36 (m, 3H), 2.59 (br, 4H), 2.87 (br, 4H), 3.19–3.4 (m, 2H), 3.47–3.54 (m, 1H), 3.6–3.69 (m, 1H), 3.86–3.9 (m, 1H), 6.81 (t, $J=7.7$ Hz, 1H), 6.89 (d, $J=8.1$ Hz, 1H), 7.02 (t, $J=7.7$ Hz, 1H), 7.12 (d, $J=7.7$ Hz, 1H), 7.18–7.27 (m, 5H). IR (KBr; cm^{-1}): 3259, 2935, 2805, 1637, 1590, 1494, 1450, 1427, 1257, 1133, 1024, 946, 767, 746, 703. MS (EI+): 421, 324, 273, 261, 244, 191, 148, 112, 70 (100%), 55.

(*R*)-7 and (*S*)-7 Compound 7 was resolved into its enantiomers by chromatography on a Chiral-Pak AD column (25 cm \times 1 cm) eluted at 4 ml/min with hexane-2-propanol-TEA (95:5:0.1 by vol.): (*S*)-7 ($[\alpha]_{\text{D}}(\text{CHCl}_3)=+63.7^\circ$), $t_{\text{R}}=7.1$ min; (*R*)-7 ($[\alpha]_{\text{D}}(\text{CHCl}_3)=-63.7^\circ$), $t_{\text{R}}=10.4$ min. HRMS for each enantiomer: required for $[\text{C}_{26}\text{H}_{36}\text{N}_3\text{O}_2]^+$ m/z 422.2807; found 422.2808.

Pharmacological screening (*R*)-6 and (*S*)-6 were submitted to the National Institute of Mental Health Psychoactive Drug Screening Program for assay of binding affinity (K_{I}) against cloned human 5-HT_{1A} receptors. (*R*)-6 was also screened in radioligand binding assays for binding affinity (K_{I}) at a wide range of other cloned (mainly human) brain receptors and transporters (5-HT_{1D}, 2A-C, 5A & 7, $\alpha_{1A,1B}$ & 2A-C, β_1 & 2, D₁₋₄, H₁ & 2, κ opiate, and SERT). Detailed protocols are available on-line for all binding assays at the NIMH-PDSP web site (<http://www.cwra.edu>). (*R*)-6 and (*S*)-6 were also screened in a [^{35}S]-GTP γ S binding assay for functional activity at cloned human 5-HT_{1A} receptors. The selective 5-HT_{1A} receptor agonist, 8-OH-DPAT, was used as the positive control with its response set to 100%. The functional assay is described at <http://www.pdsp.med.unc.edu/pdspw/functionP.php#Inh>.

Determination of *cLogP*, *cLogD*, and *LogD* values. *cLogP* and *cLogD* (at pH 7.4) values for (*R*)-6 were computed with the program Pallas 3.0 for Windows (CompuDrug; S. San Francisco; CA). *LogD* at pH 7.4 was also determined experimentally by measuring the partition of radiochemically pure [^{11}C](*R*)-6 between *n*-octanol and sodium phosphate buffer (0.15 M; pH 7.4) [23]. The aqueous layer, after octanol extraction, was analyzed by reverse phase radio-HPLC to incorporate any needed corrections for the calculation of the partition coefficient of [^{11}C](*R*)-6. Radioactivity was counted in an automatic γ -counter equipped with a NaI(Tl) well type scintillation counter (Model 1480 Wizard, Perkin Elmer Life Sciences, Boston, MA).

Radiochemistry

Production of [^{11}C](*S*)-6 or [^{11}C](*R*)-6 No-carrier-added [^{11}C]carbon dioxide (~1.4 Ci) was produced in a target of

nitrogen gas containing oxygen (1%) via the $^{14}\text{N}(p,\alpha)^{11}\text{C}$ reaction induced by irradiation with a proton beam (16 MeV; 45 μA) for 20 min from a PETtrace cyclotron (GE Medical Systems; Milwaukee, WI, USA). [^{11}C]iodomethane was produced from the [^{11}C]carbon dioxide using a PETtrace MeI MicroLab apparatus (GE). (*R*)-7 or (*S*)-7 (0.3 mg) was treated with [^{11}C]iodomethane in the presence of TBAH (0.17 M in MeOH, 4.5 μl) in anhydrous *N,N*-dimethylformamide (80 μl) within an Autoloop apparatus (Bioscan; Washington DC, USA). The reaction was allowed to proceed at RT for 5 min under a nitrogen atmosphere. The reaction mixture was then injected onto an Ultrasphere column (250 \times 10 mm; Beckman) eluted with acetonitrile–0.1 M ammonium formate (50:50 v/v) at 6 ml/min for 2 min with the acetonitrile concentration then raised to 60% over 8 min and thereafter maintained at this concentration for a further 5 min. The eluate was monitored for absorbance at 240 nm and for radioactivity. [^{11}C](*R*)-6 or [^{11}C](*S*)-6 eluted from the column with $t_{\text{R}}=9.4$ min. Product was collected and dried under reduced pressure and formulated in sterile saline (0.9% w/v; 10 ml) containing ethanol (5% w/v).

Product was analyzed with reverse phase HPLC on a Prodigy column (250 \times 4.6 mm i.d.; Phenomenex) eluted with 0.1 M ammonium formate in acetonitrile–water (60:40 v/v) at 2 ml/min. Eluate was monitored for absorbance at 240 nm and radioactivity { [^{11}C](*R*)-6 or [^{11}C](*S*)-6, $t_{\text{R}}=5.5$ min}. Radiochemical stability of formulated [^{11}C](*R*)-6 for up to 105 min was assessed with radio-HPLC. Chiral radio-HPLC was performed using a Chiral-Pak AD column (250 \times 4.6 mm i.d.; 10 μm ; Daicel) eluted with hexane-2-propanol-TEA (95:5:0.1 by vol.) at 2 ml/min with eluate monitored for radioactivity and absorbance at 254 nm: t_{RS} for (*S*)-6, (*R*)-6, [^{11}C](*S*)-7, and [^{11}C](*R*)-7 were 5.9, 9.8, 8.8, and 14.3 min, respectively.

Monkey PET imaging experiments

All animal experiments complied with the *Guide for Care and Use of Laboratory Animals* [24]. Six male rhesus monkeys (9–14.1 kg) were used for the experiments. For each PET experiment, the monkey was initially anesthetized with ketamine and then maintained under anesthesia with 1.6% isoflurane. An intravenous perfusion line, filled with saline (0.9% w/v), was used for bolus radioligand (5.29–5.90 mCi) injection. PET serial dynamic images were obtained on an Advance PET camera (GE Medical Systems). Scans were acquired for up to 90 min in 27 frames and were corrected for attenuation and scatter. PET images were co-registered to MRI scans and decay-corrected time-activity curves (TACs) were obtained for irregular volumes of interest (VOIs), namely cingulate

gyrus, frontal cortex, temporal cortex, raphe nuclei, and cerebellum. Radioactivity was normalized for injected dose and monkey weight by expression as % standardized uptake value [%SUV=(% injected dose per g) × body weight in g].

Experiments were performed in addition to the baseline (radioligand alone) experiments. In one experiment (pre-block experiment) the monkey (13.5 kg) was injected with **1** (0.5 mg/kg, i.v.) at 15 min before administration of [¹¹C](*R*)-**6** (5.44 mCi). In another (displacement experiment), the monkey (14.1 kg) was injected with **1** (0.5 mg/kg, i.v.) at 40 min after [¹¹C](*R*)-**6** (5.90 mCi).

Determination of radioligand stability, distribution between blood and plasma, and estimation of plasma free fraction

The stability of [¹¹C](*R*)-**6** in monkey blood and plasma in vitro at RT was assessed by radio-HPLC.

For the determination of radioligand distribution between rhesus monkey blood and plasma, [¹¹C](*R*)-**6** was added to blood, which was then incubated at RT for 5 min and centrifuged at 3,000 *g* at RT for 20 min. The pellet and supernatant plasma were each counted for radioactivity.

For the determination of radioligand binding to blood proteins, [¹¹C](*R*)-**6** was added to monkey plasma. Samples (200 μl) were placed in triplicate ‘Amicon’ filtration units and centrifuged at 5,000 *g* at RT for 20 min. Top and bottom components of the filtration unit and a known volume of filtrate were then counted for radioactivity [25].

Emergence of radiometabolites in plasma

An intra-arterial line was used to obtain blood samples from three rhesus monkeys while under baseline PET study after injection of [¹¹C](*R*)-**6**. Samples were drawn into heparinized syringes at precise times every 15 s up to 120 s and 3, 5, 20, 40, 60, and 90 min after radioligand injection. Each blood sample was centrifuged for 2 min at 1,800 *g* (Centra CL2; Thermo IEC). Then each generated plasma sample was diluted 1.5-fold with acetonitrile and agitated. The sample was then diluted 9% with water and mixed again. Radioactivity was measured with a calibrated automatic well-type γ-counter with an electronic window set between 360 and 1,800 keV and decay corrected to time of dose administration. Total plasma activity concentration was expressed as dpm/ml. The plasma-acetonitrile samples were centrifuged at 9,400 *g* for 2 min and supernatant liquids analyzed by radio-HPLC with a Novapak C18 column (RCM-100) eluted with methanol–water–TEA (80:20:0.1 by vol.) at 1.5 ml/min. The HPLC system was equipped with an in-line UV absorbance (λ=245 nm) and a flow-through radioactivity detector. Data were stored and analyzed on a PC using the software “Bio-ChromeLite”.

Radiochromatograms were decay corrected to the sample injection time.

Structural elucidation of plasma and urinary radiometabolites

A rhesus monkey (11.85 kg) was injected with [¹¹C](*R*)-**6** (4.52 mCi; radiochemical purity 99.8%; specific radioactivity 1.51 Ci/μmol; carrier (*R*)-**6**: 1.3 μg; 3.0 nmol) in saline (0.9% w/v; 10 ml) containing ethanol (5% w/v) through an intravenous cannula. Urine was sampled continuously through a urethral catheter. Urine that had accumulated up to 15 min after radioligand injection was sampled for radio-HPLC analysis and the remainder stored at –70°C for full radioactive decay to provide background data for subsequent LC-MS and MS-MS analysis. At 15 min after radioligand injection, one arterial blood sample was also withdrawn for radio-HPLC analysis. At 40 min after radioligand injection, (*R*)-**6** (10 mg; 23 μmol) in saline (0.9% w/v; 10 ml) containing ethanol (5% w/v) was administered to the monkey. Another blood sample was collected for radio-HPLC analysis 45 min later. Finally, at the end of the study (2 h from radioligand injection), the accumulated urine was sampled for radio-HPLC, LC-MS, and MS-MS analysis.

Blood samples were centrifuged at 1,800 *g* for 2 min to separate plasma. Plasma (450 μl) or urine samples (100 μl) were then placed in acetonitrile (700 μl) that had been spiked with carrier (*R*)-**6**. These samples were mixed, diluted 10% with water, and mixed again. Plasma-acetonitrile or urine-acetonitrile mixtures were counted in the γ-counter. Samples to be analyzed by radio-HPLC were centrifuged at 9,400 *g* for 2 min. The clear supernatant liquids were injected into the radio-HPLC through a nylon filter (pore size: 0.45 nm). Radio-HPLC was performed as described above for the analysis of plasma samples during PET experiments, but with methanol–water–TEA (75/25/0.1; by vol.) as mobile phase. Precipitates were counted in the γ-counter to enable calculation of recovery of radioactivity into supernatant liquids after acetonitrile treatment.

For LC-MS-MS, a sample of urine (1 ml) was taken, mixed with acetonitrile (2 ml), left for 1 h at 4°C, and centrifuged (5,000 *g* for 5 min). The clear supernatant liquid was evaporated to dryness on a SpeedVac evaporator (Thermo Electron Corp.; Milford, MA). The residue was dissolved in water (150 μl) and a sample (5 μl) introduced into an LC-MS instrument (LCQ Deca; Thermo Electron Corp., San Jose, CA), equipped with a reverse phase HPLC column (Synergi Fusion-RP; 4 μm; 150×2 mm; Phenomenex) that had been pre-equilibrated with a mixture of 80% *aq.* ammonium formate (10 mM) (A) and 20% acetonitrile (B). The metabolites of (*R*)-**6** were eluted at 150 μl/min with a linear gradient, reaching 20% A and 80% B over

6 min followed by isocratic elution for 6 min. The LC effluent was diverted from waste into the electrospray module of the LC-MS at 2.5 min after the start of analysis. At the end of analysis, the mobile phase composition was returned to 80% A and 20% B over 1 min at a flow rate of 250 $\mu\text{l}/\text{min}$. The column was allowed to equilibrate for 3 min before starting another analysis.

For electrospray ionization the settings were: spray voltage, 4.5 kV; sheath gas (N_2) flow rate, 45 units; capillary voltage, 20 V; capillary temperature, 260°C. In the full scan MS acquisition mode, the instrument method was set up to detect ions in the range m/z 150–750. For MS-MS experiments, the molecular ion of (*R*)-**6** or a metabolite of interest was isolated with a mass width of 1.5 a.m.u. and dissociated in the ion trap at a collision energy level of 30%.

Results

Chemistry

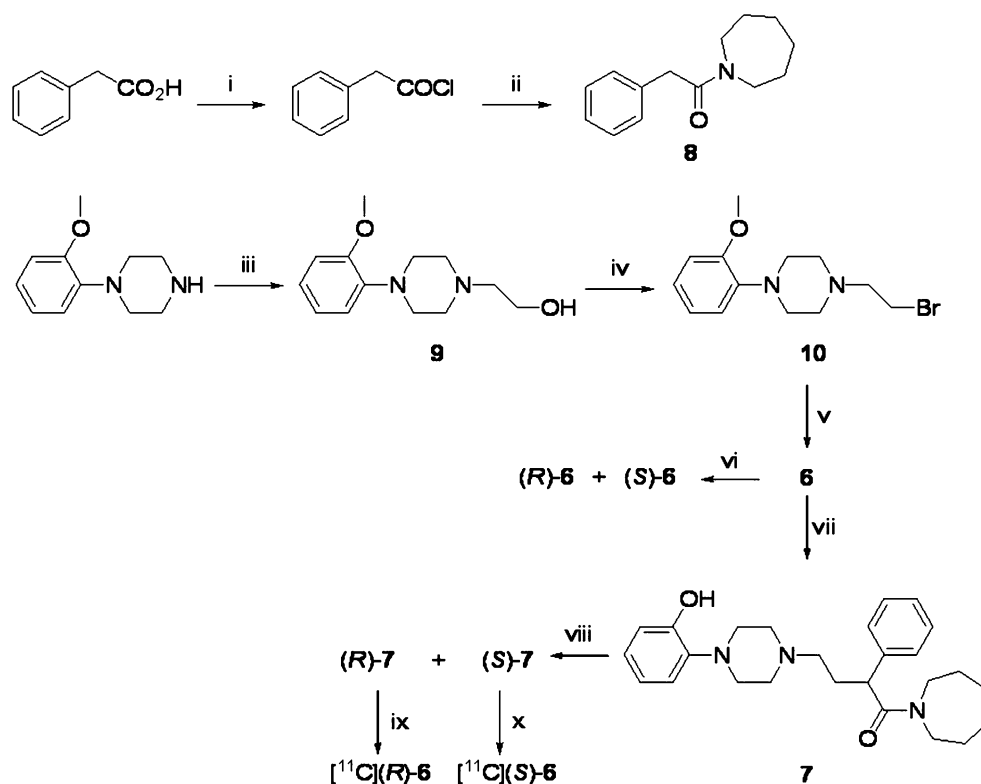
The amide **8** was obtained in two steps in high overall yield (93%) and the bromo compound **10** also in two steps in high overall yield (92%) (Fig. 2). These were converted into **6** in moderate yield (48%), which was then completely

resolved ($\alpha=1.69$) into its enantiomers on a Chiral-Pak AD column. Ligand **6** was converted efficiently (83%) into the phenol **7** by treatment with aluminum chloride in refluxing benzene and also completely resolved ($\alpha=1.73$) into its enantiomers on a Chiral-Pak AD column. (*R*)-**7** and (*S*)-**7** were free of starting material **6**.

Pharmacological screening

In two separate and identical assays, (*R*)-**6** was found to have a K_I of 0.60 ± 0.06 ($n=3$) and 1.88 ± 0.41 ($n=3$) nM at cloned human 5-HT_{1A} receptors. K_I values (nM) at other receptors in descending order were found to be: β_2 (>10,000), H₂ (3,296), SERT ($3,269\pm 511$), 5-HT_{2C} (1,682), κ opiate (1,609), α_{2B} (1,476), α_{2A} (1,311), β_1 (770), D₁ (732), 5-HT_{1B} (445 ± 116), H₁ (335), 5-HT_{5A} (306), α_{1B} (222), 5-HT_{2A} (148 ± 31), α_{2C} (92), 5-HT₇ (65.4 ± 12.8), D₂ (34.5 ± 23.6), D₄ (15.6 ± 1.5), α_{1A} (10.4 ± 0.57), 5-HT_{1D} (9.49 ± 1.91), 5-HT_{2B} (7.2 ± 1.1), and D₃ (5.1 ± 0.06). (*S*)-**6** was found to have a K_I of 0.48 ± 0.03 ($n=3$) at 5-HT_{1A} receptors (compared to 1.88 nM for (*R*)-**6** in the same assay experiment). In the functional assay (*R*)-**6** was found to be an antagonist at human cloned 5-HT_{1A} receptors, while (*S*)-**6** was found to be a weak partial agonist with a maximal response of 16.75% of that of 8-OH-DPAT and an EC₅₀ of 3.1 nM (cf. 39.6 nM for 8-OH-DPAT).

Fig. 2 Synthesis of enantiomers of **6**, **7**, and [¹¹C]**6**. Reagents and conditions: (i) SOCl₂; (ii) cyclohexylimine, TEA, RT, overnight; (iii) 2-bromoethanol, K₂CO₃, reflux overnight; (iv) Ph₃P, Br₂, RT 1 h; (v) **8**, LDA, RT overnight; (vi) chiral chromatography; (vii) AlCl₃, benzene, reflux, 48 h; (viii) chiral chromatography; (ix and x) ¹¹CH₃I, TBAH, DMF, RT, 5 min



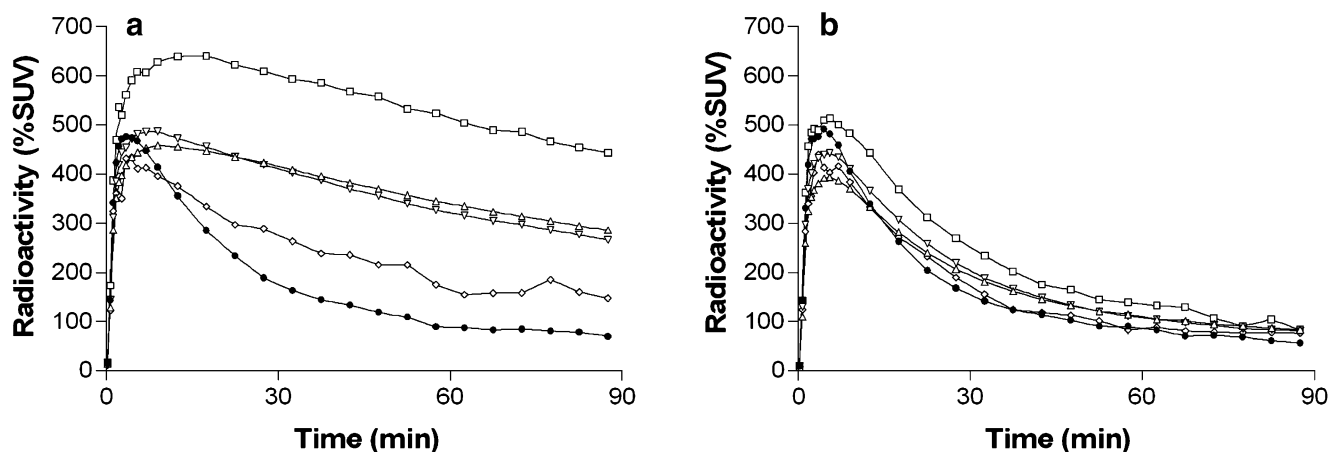


Fig. 3 Uptake of radioactivity (%SUV) into VOIs after administration of [^{11}C](R)-6 (5.79 mCi) (a) or [^{11}C](S)-6 (5.29 mCi) (b) to the same rhesus monkey (10.5 kg). Key: \square , cingulate gyrus; ∇ , temporal cortex; Δ , frontal cortex; \diamond , raphe nuclei; \bullet , cerebellum

cLogP, cLogD, and LogD values

(R)-6 was found to have *cLogD* at pH 7.4 and *cLogP* values of 2.61 and 3.96, respectively. The experimentally determined *LogD* value at pH 7.4 was 3.16 ± 0.35 (mean \pm SD; $n=6$).

Radiochemistry

The average yield of [^{11}C](R)-6 was 96 mCi (range 43–172 mCi, $n=7$) at 35 min from the end of radionuclide production. The average overall decay-corrected yield from [^{11}C]carbon dioxide was estimated to be about 33%. The radiochemical purity was found to be greater than 99% and the average specific radioactivity 3.18 Ci/ μmol at the end of radiosynthesis (range 2.57–3.75 Ci/ μmol , $n=7$).

[^{11}C](S)-6 (52.2 mCi) was produced once in >99% radiochemical purity with a specific radioactivity of 2.17 Ci/ μmol .

Each radioligand product was radiochemically and enantiomerically stable at RT for at least 105 min after preparation.

Monkey PET imaging

After injection of [^{11}C](R)-6 into a rhesus monkey, there was a rapid and high uptake of radioactivity into all examined VOIs, with highest uptake in cingulate gyrus (641% SUV after 17.5 min). The distribution of radioactivity then became more heterogeneous, with slow washout of radioactivity from VOIs with high 5-HT_{1A} densities, such as cingulate gyrus, frontal cortex, temporal cortex, and raphe nuclei, and fast washout of radioactivity from the almost receptor-devoid cerebellum (Fig. 3a). The ratio of radioactivity concentration in cingulate gyrus to that in cerebellum reached 6.4 at 87.5 min after injection (Fig. 4a). The corresponding ratios for frontal cortex, temporal cortex, and raphe nuclei were 4.1, 3.8, and 2.1, respectively. In the experiment in which **1** (0.5 mg/kg) was administered at 15 min before [^{11}C](R)-6, the distribution of radioactivity became almost homogeneous throughout brain at about 15 min after radioligand injection (Fig. 5). In the experiment in which **1** (0.5 mg/kg) was administered at

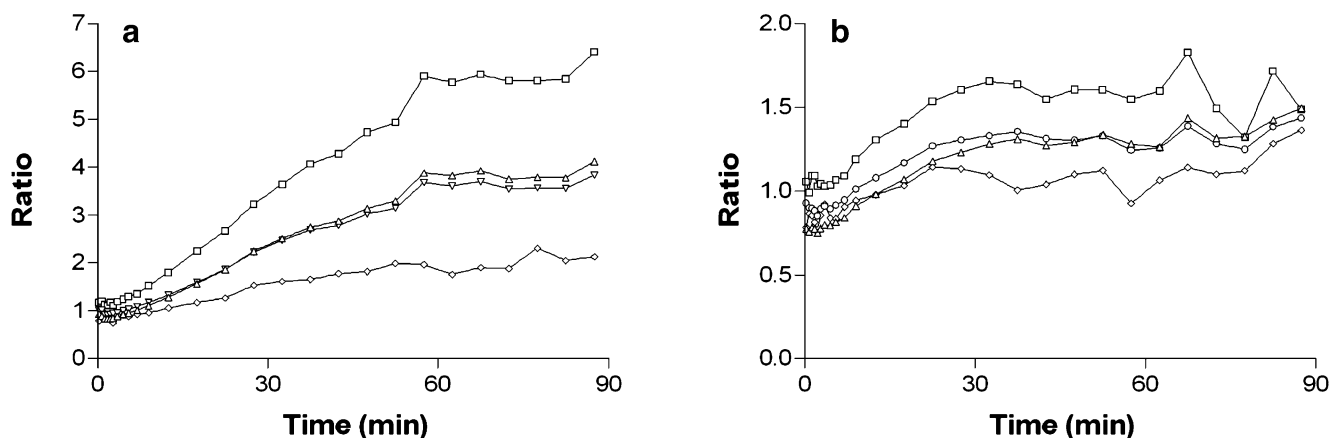


Fig. 4 Time course of ratios of radioactivity concentration in 5-HT_{1A} receptor-rich VOIs to that in receptor-devoid cerebellum after administration of [^{11}C](R)-6 (a) or [^{11}C](S)-6 (b) to rhesus monkey

(as detailed under legend to Fig. 3). Key: \square , cingulate gyrus; ∇ , temporal cortex; Δ , frontal cortex; \diamond , raphe nuclei

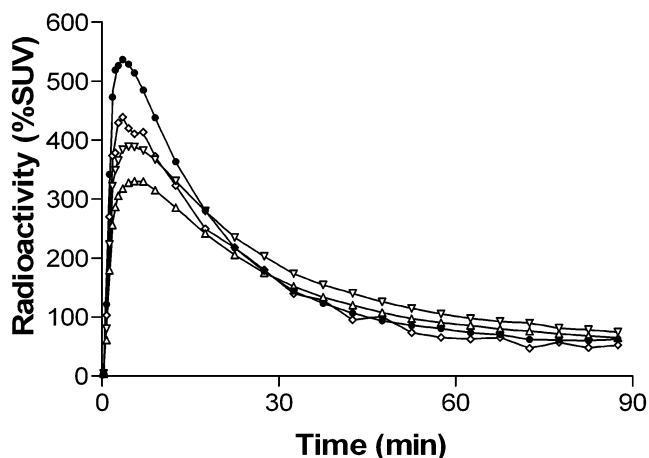


Fig. 5 Uptake of radioactivity (%SUV) into brain VOIs after administration of [^{11}C](R)-6 (5.44 mCi, i.v.) at 15 min after administration of **1** (0.5 mg/kg, i.v.) to rhesus monkey (13.5 kg). Key: ∇ , temporal cortex; Δ , frontal cortex; \diamond , raphe nuclei; \bullet , cerebellum

40 min after injection of [^{11}C](R)-6, the radioactivity levels in 5-HT_{1A} receptor-rich regions decreased immediately, resulting in tissue to cerebellum radioactivity ratios of less than 2 at 87.5 min after radioligand injection (Fig. 6).

PET scans of brain (averaged between 30 and 90 min) obtained after injection of [^{11}C](R)-6 into rhesus monkey, and co-registered with MRI scans, showed a distribution of radioactivity consistent with a large proportion of binding to 5-HT_{1A} receptors (Fig. 7). Corresponding scans from the preblock experiment showed a uniformly low radioactivity concentration across brain.

The behavior of [^{11}C](S)-6 was very different to its antipode. After injection of [^{11}C](S)-6 into monkey, the uptake and washout of radioactivity from cerebellum was almost identical to that for [^{11}C](R)-6 in the same monkey

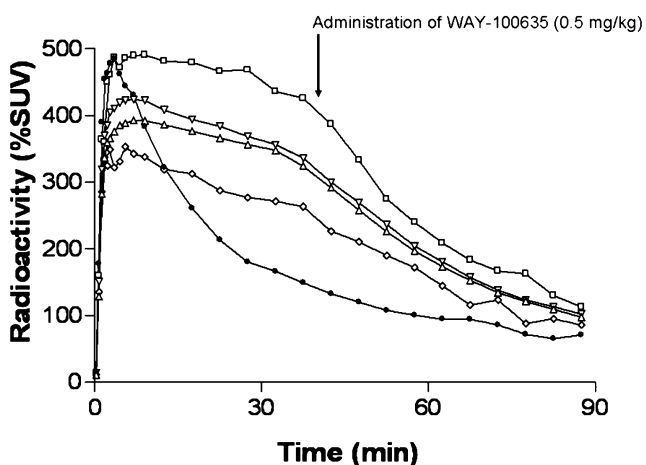


Fig. 6 Uptake of radioactivity (%SUV) into brain VOIs after administration of [^{11}C](R)-6 (5.90 mCi, i.v.) followed 40 min later with **1** (0.5 mg/kg, i.v.) into rhesus monkey (14.1 kg). Key: \square , cingulate gyrus; ∇ , temporal cortex; Δ , frontal cortex; \diamond , raphe nuclei; \bullet , cerebellum

(Fig. 3b). Although radioactivity was taken up in 5-HT_{1A} receptor-rich regions to a level similar to that in cerebellum, this radioactivity decreased rapidly. Ratios of radioactivity in these regions to that in cerebellum became less than 2 at 87.5 min (Fig. 4b).

Radioligand, stability, distribution between blood and plasma, and plasma free fraction

[^{11}C](R)-6 was stable in monkey blood and plasma in vitro for at least 30 and 120 min, respectively, at RT. The radioligand distributed 73.7% to plasma and 27.3% to cells while the protein-free fraction of radioligand in plasma was $2.9 \pm 0.8\%$ (mean, $n=3$).

Emergence of radiometabolites in plasma

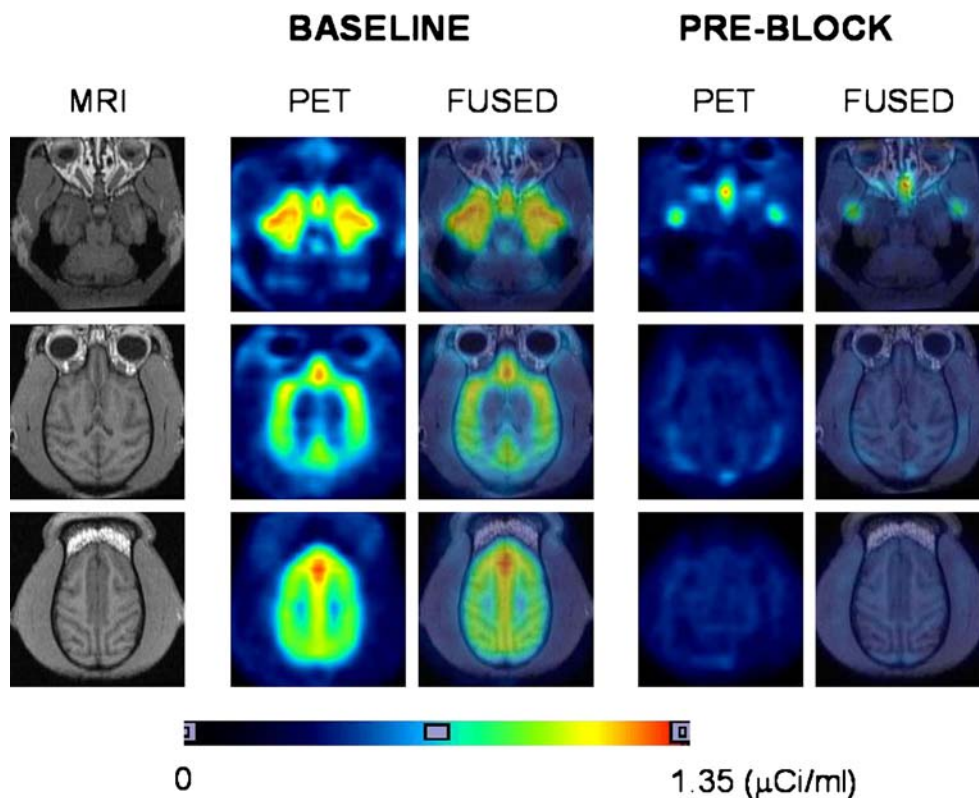
After administration of [^{11}C](R)-6 to monkey, total radioactivity and parent radioligand cleared rapidly from arterial plasma (Fig. 8). In the reverse phase radio-HPLC analysis, four major radioactive peaks were detected in each plasma analyte; one represented parent radioligand ($t_R=5.4 \pm 0.6$ min) and the others represented less lipophilic radiometabolite fractions ($t_{RS}=2.1 \pm 0.7$, 3.3 ± 0.8 , and 4.8 ± 1.0 min for radiometabolites A, B, and C, respectively) ($n=33$ plasma determinations in two monkeys). The average total radioactivity represented by [^{11}C](R)-6 was $81.0 \pm 4.3\%$ at 5 min, which decreased to $14.0 \pm 1.5\%$ at 60 min after injection ($n=3$ monkeys) (Fig. 9). The intermediate region of the radiochromatograms, represented by the minor radiometabolites B and C, was always less than 10% of the total plasma radioactivity (Fig. 10). Radiometabolite A represented the majority of radioactivity in plasma after 20 min (Fig. 10).

Structural elucidation of plasma and urinary radiometabolites

In this experiment, one major and two minor radiometabolite fractions were detected with radio-HPLC in monkey plasma at 15 and 60 min after [^{11}C](R)-6 injection. The major radiometabolite fraction eluted near the void volume (4.3 ml; $t_R=2.9$ min) while the minor radiometabolite fraction eluted just after ($t_R \sim 4$ min) and before parent radioligand ($t_R \sim 10.5$ min). The minor radiometabolite fraction was incompletely resolved from the major radiometabolite fraction. Radiometabolites with the same retention times as those in plasma were detected in urine by radio-HPLC. Radioactivity from parent radioligand was not detected in urine.

At 15 min after radioligand injection, the urine (39 ml) collected from the monkey contained 1.8% of the injected radioactive dose. The 60-min urine sample (72 ml) contained 13.1% of the injected dose, equating to 3 μmol of radiometabolites.

Fig. 7 Average PET scans of rhesus monkey brain obtained between 30 and 90 min after administration of [^{11}C](*R*)-**6** (4.70 mCi, i.v.) alone (baseline condition; 2nd column from left) and in the same monkey under preblock conditions (4th column from left) [**1** (0.5 mg/kg, i.v.) injected at 15 min before radioligand (5.40 mCi)]. PET data were acquired with the monkey (13.5 kg) under 1.6% isoflurane anesthesia. The corresponding MRI scans are shown in the 1st column from the left. Fused PET-MRI scans under baseline and preblock conditions are shown in the 3rd and 5th columns from the left, respectively. Scans were taken axially at the level of raphe nuclei and medial temporal cortex (upper row), the frontal temporal region (middle row), and the anterior cingulate and parietofrontal region (lower row)



LC-MS analysis of the 60-min urine sample detected parent (*R*)-**6** ($t_{\text{R}}=10.5$ min) with m/z 436, one metabolite ($t_{\text{R}}=10.33$ min) with m/z 450, two metabolites ($t_{\text{R}}=8.78$ and 8.97 min) with m/z 452, one metabolite ($t_{\text{R}}=7.21$ min) with m/z 330, and one metabolite ($t_{\text{R}}=6.65$ min) with m/z 468. MS-MS of (*R*)-**6** in urine gave a major product (fragment) ion with m/z 244 and a minor product ion with $m/z=337$. Product ions from MS-MS of the parent molecular ions of (*R*)-**6** and the detected metabolites are shown in Fig. 11.

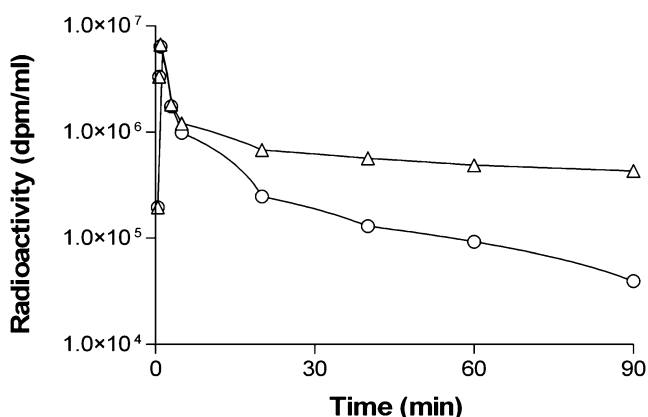


Fig. 8 Clearance of total radioactivity (Δ) and unchanged [^{11}C](*R*)-**6** (\circ) from arterial plasma after administration of [^{11}C](*R*)-**6** (6.26 mCi) to rhesus monkey (16.6 kg)

Discussion

Chemistry

The synthesis of **6** has been reported by different routes, including in the final step, alkylation of an amide intermediate [20], coupling of an acid with cyclohexylimine [26, 27], or reaction of 2-methoxy-phenyl-piperazine with a homochiral aldehyde [28]. The *R*-enantiomer of **6** has been obtained by separation of dibenzyl-D-tartrate salts of the

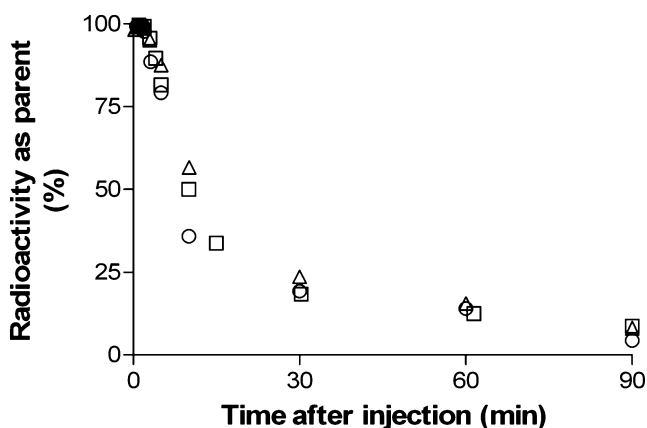


Fig. 9 Time course of radioactivity in plasma represented by parent radioligand after injection of [^{11}C](*R*)-**6** into rhesus monkeys. Data are shown for three individual monkeys. The remainder of radioactivity consisted of more polar radiometabolites (see Fig. 10)

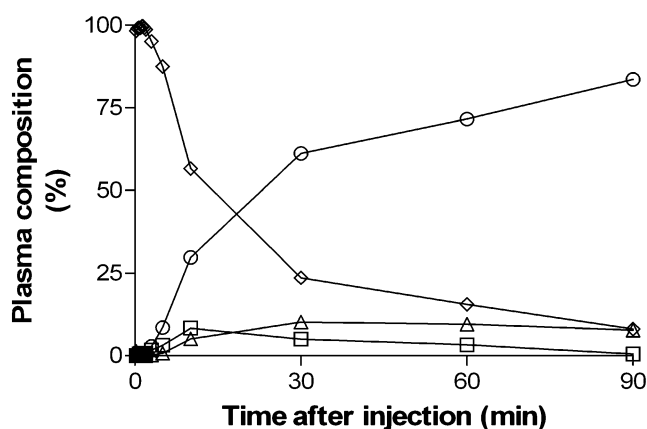


Fig. 10 Time course of radioactive species in plasma after injection of [^{11}C](*R*)-**6** into rhesus monkey. \circ , radiometabolite A ($t_R=2.1\pm 0.7$ min); Δ , radiometabolite B ($t_R=3.3\pm 0.8$ min); \square , radiometabolite C ($t_R=4.8\pm 1.0$ min); \diamond , parent [^{11}C](*R*)-**6** ($t_R=5.5\pm 0.6$ min)

racemate [20] or by asymmetric synthesis [28]. The asymmetric synthesis is multistage from (*S*)-mandelic acid and low yielding (<15%), but has served to establish the absolute configurations of the enantiomers. We adapted the much shorter method based on alkylation [20] to use alkyl bromide instead of alkyl chloride and obtained racemic **6** in moderate overall yield (Fig. 2). The yield of the alkylation reaction with the bromide (43%) was much greater than that reported with the chloride (~10%). We also found that **6** was readily resolved into its enantiomers by chiral chromatography on a useful multi-milligram scale, as was the derived *O*-desmethyl compound **7**.

Pharmacological screening

(*R*)-**6** showed high affinity ($K_1=0.60$ and 1.88 nM in two separate assays) for 5-HT_{1A} receptors with high selectivity (>50-fold) over binding to a wide array of other binding sites (receptors or transporters). Notably, (*R*)-**6** was found to

be less than 50-fold selective for binding to 5-HT_{1A} receptors over D₄ (26-fold), α_{1A} (17-fold), 5-HT_{1D} (16-fold), and D₃ (ninefold) receptors. However, these off-target receptors appear to exist in human brain at lower concentrations (e.g. D₄ (≤ 68 nM) [29], α_{1A} (≤ 40 nM) [30], and D₃ (≤ 3 nM) [31]) than 5-HT_{1A} receptors (≤ 200 nM) [30, 32, 33]. Consequently, their binding potentials (B_{max}/K_D) are probably about 50-fold lower than that of the targeted 5-HT_{1A} receptors. Hence, any brain 5-HT_{1A} receptor-specific binding obtained with (*R*)-[^{11}C]**6** in vivo is unlikely to be significantly contaminated with signal from other binding sites.

Previously, the IC₅₀ value of (*S*)-**6** for binding to 5-HT_{1A} receptors has been reported to be 1 nM, threefold higher than that of the racemate [20]. We found (*S*)-**6** and (*R*)-**6** to have very close K_1 values, with the *S*-enantiomer showing slightly higher affinity in the same assay experiment. The enantiomers exhibited a clear difference in intrinsic activity in the functional assay with the *R*-enantiomer behaving as an antagonist and the *S*-enantiomer as a weak partial agonist.

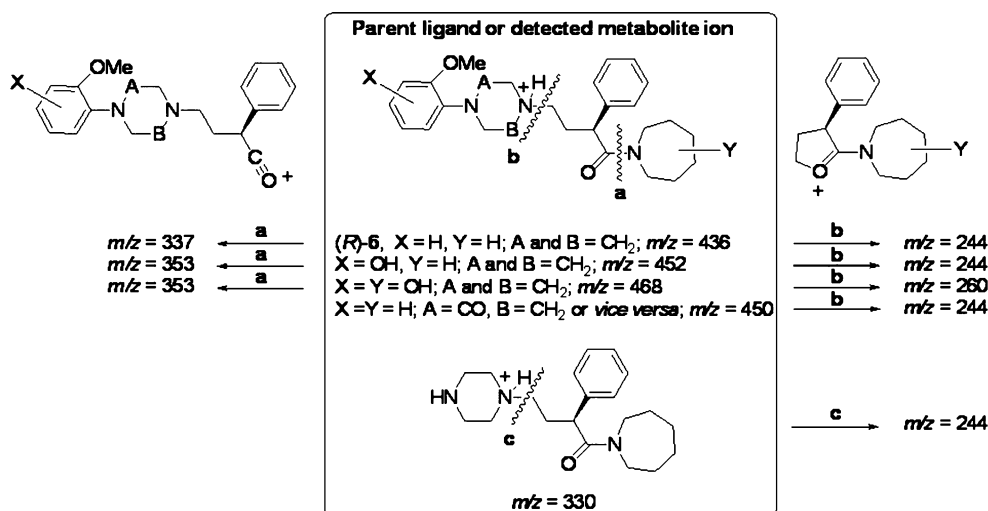
cLogP, *cLogD*, and *LogD* values

The *cLogD* value (2.61) is just outside the mean minus the standard deviation of the experimentally determined value (3.16–0.35=2.81), indicating that the Pallas program is quite accurate for calculations on this type of structure. The *cLogP* value of 3.96 is above the range generally considered optimal for good blood-brain barrier penetration [34, 35]. Nevertheless, [^{11}C](*R*)-**6** and [^{11}C](*S*)-**6** show acceptably high penetration into rhesus monkey brain (see below).

Radiochemistry

[^{11}C](*R*)-**6** and [^{11}C](*S*)-**6** were prepared by methylation with [^{11}C]iodomethane under identical strongly basic

Fig. 11 Molecular ions from (*R*)-**6** and metabolites detected in monkey urine by LC-MS, showing their paths (a–c) to product ions in MS-MS



reaction conditions (Fig. 2). These conditions do not cause racemization and they are simple and reliable.

Monkey PET imaging

The uptake of each radioactivity into VOIs became high (in the range 380–650% SUV) soon after injection of [^{11}C](*S*)-**6** or [^{11}C](*R*)-**6** into rhesus monkey (Fig. 3). This brain radioactivity uptake is comparable to that observed with [*carbonyl*- ^{11}C]**1** in cynomolgus monkey [36], and very acceptable for a prospective PET radioligand. For each radioligand, following maximal uptake of radioactivity into receptor-poor cerebellum, radioactivity in this region decreased to a very low level over the remaining time span of the experiment (Fig. 3). The cerebellar curves for each radioligand in the same monkey are virtually superimposable, showing absence of stereoselectivity for binding in this region, an observation consistent with non-specific binding only. However, the kinetics of radioactivity in VOIs rich in 5-HT_{1A} receptors was very different between radioligands (Fig. 3); radioactivity washed out much more slowly for the *R*-enantiomer than for the *S*-enantiomer. For each radioligand the rank order of radioactivity concentration during the washout phase was in the expected order of brain regional 5-HT_{1A} receptor concentration (i.e. cingulate gyrus > frontal cortex \approx temporal cortex > raphe nuclei > cerebellum). Ratios of radioactivity in receptor-rich VOIs to that in cerebellum were much higher for the *R*-enantiomer (maximally 6.4 in cingulate gyrus at 87.5 min) than for the *S*-enantiomer (maximally 1.83 in cingulate gyrus at 67.5 min) (Fig. 4). Hence, both radioligands appear to give receptor-specific signals in baseline experiments, but of

very different magnitudes. This difference is not easily explained, since each enantiomer has almost identical affinity, the same lipophilicity, and the same non-specific binding in cerebellum (implying very similar input of radioactive species into brain). However, the two enantiomers were found to differ in intrinsic activity, with the *R*-enantiomer (the more effective for *in vivo* imaging) behaving as an antagonist and the *S*-enantiomer behaving as a weak partial agonist at 5-HT_{1A} receptors. Agonist radioligands with similar pairings of binding affinities and lipophilicities to antagonist radioligands are historically much less successful as PET radioligands for 5-HT_{1A} receptors [4]; generally the agonists give low or no receptor-specific binding *in vivo*.

Antagonists are expected to bind to the full population of 5-HT_{1A} receptors, while agonists are expected to bind only to receptors in the high-affinity G-protein-coupled state, a subpopulation of receptors. Hence, [^{11}C](*S*)-**6** may have some potential for imaging this subpopulation and this possibility deserves future investigation.

We selected [^{11}C](*R*)-**6** for more detailed evaluation since it gave much greater signals (ratios of radioactivity in 5-HT_{1A} receptor-rich regions to that in cerebellum) in a baseline experiment than [^{11}C](*S*)-**6** (Fig. 4). PET experiments in which a monkey was dosed with the antagonist **1** before injection of [^{11}C](*R*)-**6** or in which **1** was given at 40 min after radioligand injection confirmed receptor binding selectivity *in vivo*. In the preblock experiment, radioactivity in all VOIs almost matched that in cerebellum between 20 and 87.5 min after radioligand injection (Fig. 5), while in the displacement experiment radioactivity was reduced almost to that in cerebellum at 87.5 min

Fig. 12 Metabolic pathways for (*R*)-**6** in rhesus monkey

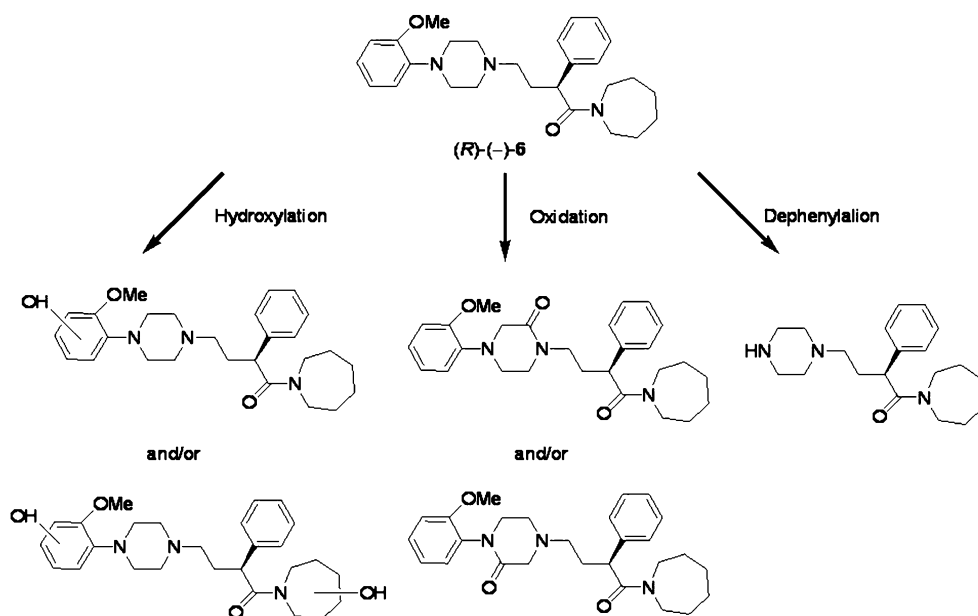


(Fig. 6). PET images acquired between 30 and 90 min after radioligand administration under baseline conditions and subsequently fused with MRI scans showed radioactivity distributed predominantly according to the known distribution of 5-HT_{1A} receptors (Fig. 7). In scans from the preblock experiment, radioactivity levels were greatly diminished throughout the brain (Fig. 7).

Radioligand stability, distribution between blood and plasma, and protein binding

[¹¹C](*R*)-6 was stable in monkey blood and plasma *in vitro* and was taken up moderately in blood cells, with the vast majority staying in plasma. Therefore, once radioactive blood samples were drawn, no metabolism would have occurred *ex vivo*. The detection of radiometabolites in such plasma samples could only be the result of the metabolizing organs *in vivo*. We did not investigate which organs were responsible for this metabolism. The protein-free fraction in plasma was 2.9±0.8%, as determined in triplicate in each of three studied monkeys, and was therefore measurable with reasonable accuracy, if required as a parameter for biomathematical modeling.

Emergence of radiometabolites in plasma

The clearance of total radioactivity and parent [¹¹C](*R*)-6 radioligand from arterial plasma was rapid (Fig. 8). The emergence of radiometabolites in plasma was also rapid (Fig. 9). Parent radioligand represented on average 82.8% and 14% of radioactivity in plasma at 5 and 60 min, respectively. As indicated by their shorter retention times on reverse phase HPLC, all radiometabolites were much less lipophilic than [¹¹C](*R*)-6. The least lipophilic radiometabolite became the dominant radioactive species in plasma from about 20 min after radioligand injection (Fig. 10).

Structural elucidation of urinary and plasma metabolites

LC-MS-MS analysis detected several metabolites of (*R*)-6 (Fig. 11) that are deduced to arise from aromatic and aliphatic hydroxylation, oxidation to ketone, and *N*-dephenylation of (*R*)-6 (Fig. 12). The applied technique did not allow the relative proportions of each metabolite in urine to be determined. Metabolites of [¹¹C](*R*)-6 retaining an *O*-methyl group would be radioactive in urine and plasma, but their ability to penetrate the blood-brain barrier in monkey remains unknown. No products arising from hydrolysis of the amide bond in (*R*)-6 or demethylation were found in monkey. With the exception of piperidine ring oxidation, the pathways found for metabolism of [¹¹C](*R*)-6 in rhesus monkey have also been observed in rat [37].

Conclusion

[¹¹C](*R*)-6 may be prepared effectively by the widely established technique of methylation of a phenol group with [¹¹C]iodomethane. No racemization occurs during this process. [¹¹C](*R*)-6 is an effective antagonist radioligand for imaging 5-HT_{1A} receptors in monkey brain since it shows high brain uptake, a high degree of specific binding to 5-HT_{1A} receptors, and a rate of clearance of radioactivity from plasma and brain regions favorable to successful biomathematical modeling. (A detailed study of the biomathematical modeling of PET data obtained with [¹¹C](*R*)-6 in rhesus monkey is now described elsewhere [38]). The amide bond of this radioligand resists hydrolysis in monkey *in vivo*. By contrast, the similar affinity antipode, [¹¹C](*S*)-6, is a weak partial agonist and shows high early uptake into brain, but very much lower specific binding to 5-HT_{1A} receptors. [¹¹C](*R*)-6 is not metabolized by hydrolysis, but by other pathways including dephenylation, oxidation, and aromatic and aliphatic hydroxylation. This radioligand merits further evaluation. An exploratory IND has been approved for [¹¹C](*R*)-6 by the FDA and studies will commence to investigate the effectiveness of this radioligand in human subjects.

Acknowledgements This work was supported by the Intramural Research Program of the National Institutes of Health (National Institute of Mental Health; project # Z01-MH-002852-01). An early phase of this project was also supported by the Human Frontier Science Program Organization (grant # RG 235/98). We are grateful to the National Institute of Mental Health Psychoactive Drug Screening Program (Director Dr. Bryan L. Roth) for performing binding and functional assays, and to Mr Jinsoo Hong for assistance in radioligand production.

References

1. Pike VW, McCarron JA, Hume SP, Ashworth S, Opacka-Juffry J, Osman S, et al. Pre-clinical development of a radioligand for studies of central 5-HT_{1A} receptors *in vivo*—[¹¹C]WAY-100635. *Med Chem Res* 1994;5:208–27.
2. Farde L, Ginovart N, Ito H, Lundkvist C, Pike VW, McCarron JA, et al. PET-characterization of [¹¹C]WAY-100635 binding to 5-HT_{1A} receptors in the primate brain. *Psychopharmacology* 1997;133:196–202.
3. Pike VW, McCarron JA, Lammertsma AA, Osman S, Bench CJ, Grasby PM, et al. Exquisite delineation of 5-HT_{1A} receptors in human brain with PET and [¹¹C]WAY-100635. *Eur J Pharmacol* 1996;301:R5–7.
4. Pike VW, Halldin C, Wikström HV. Radioligands for the study of 5-HT_{1A} receptors *in vivo*. *Progr Med Chem* 2000;38:189–247.
5. Andrée B, Halldin C, Thorberg S, Sandell J, Farde L. Use of PET and the radioligand [¹¹C]WAY-100635 in psychotropic drug development. *Nucl Med Biol* 2000;27:515–21.
6. Osman S, Lundkvist C, Pike VW, Halldin C, McCarron JA, Swahn CG, et al. Characterization of the radioactive metabolites of the 5-HT_{1A} receptor radioligand, [*O*-methyl-¹¹C]WAY-100635, in monkey and human plasma by HPLC: comparison of the

- behaviour of an identified radioactive metabolite with parent radioligand in monkey using PET. *Nucl Med Biol* 1996;23:627–34.
7. Osman S, Lundkvist C, Pike VW, Halldin C, McCarron JA, Swahn CG, et al. Characterization of the appearance of radioactive metabolites in monkey and human plasma from the 5-HT_{1A} receptor radioligand, [*carbonyl*-¹¹C]WAY-100635—explanation of high signal contrast in PET and an aid to biomathematical modeling. *Nucl Med Biol* 1998;25:215–23.
 8. Mathis CA, Simpson NR, Mahmood K, Kinahan PE, Mintun MA. [¹¹C]WAY-100635—a radioligand for imaging 5-HT_{1A} receptors with positron emission tomography. *Life Sci* 1994;55:PL403–7.
 9. McCarron JA, Turton DR, Pike VW, Poole KG. Remotely-controlled production of the 5-HT_{1A} receptor radioligand, [*carbonyl*-¹¹C]WAY-100635, via ¹¹C-carboxylation of an immobilized Grignard reagent. *J Label Compd Radiopharm* 1996;38:941–53.
 10. Hwang D-R, Simpson NR, Montoya J, Mann JJ. An improved one-pot procedure for the preparation of [¹¹C-carbonyl]-WAY100635. *Nucl Med Biol* 1999;26:815–9.
 11. Andrée B, Olsson J, Halldin C, Pike VW, Farde L. The PET radioligand [*carbonyl*-¹¹C]desmethyl-WAY-100635 binds selectively to 5-HT_{1A} receptors and induces a higher radioactive signal than [*carbonyl*-¹¹C]WAY-100635 in the living brain. *J Nucl Med* 2002;43:292–303.
 12. Pike VW, Halldin C, McCarron JA, Lundkvist C, Hirani E, Olsson H, et al. [*carbonyl*-¹¹C]Desmethyl-WAY-100635 (DWAY) is a potent and selective radioligand for central 5-HT_{1A} receptors in vitro and in vivo. *Eur J Nucl Med* 1998;25:338–46.
 13. Itsenko O, Kihlberg T, Blom E, Långström B. One step synthesis of [*carbonyl*-¹¹C]WAY-100635. *J Label Compd Radiopharm* 2005;48:S135.
 14. Carson RE, Toczek MT, Lang LX, Fraser C, Spanaki MV, Ma Y, et al. Human functional imaging with the 5-HT_{1A} ligand ¹⁸F-FCWAY. *J Nucl Med* 2002;198(Suppl S):55P.
 15. Passchier J, Van Waarde A, Pieterman RM, Elsinga PH, Pruijm J, Hendrikse HN, et al. In vivo delineation of 5-HT_{1A} receptors in human brain. *J Nucl Med* 2000;41:1830–5.
 16. Passchier J, Van Waarde A, Vaalburg W, Willemsen ATM. On the quantification of [¹⁸F]MPPF binding to 5-HT_{1A} receptors in the human brain. *J Nucl Med* 2001;42:1025–31.
 17. Sanabria-Bohorquez SM, Biver F, Damhaur P, Wikler D, Veraart C, Goldman S. Quantification of 5-HT_{1A} receptors in human brain using p-MPPF kinetic modeling and PET. *Eur J Nucl Med Mol Imaging* 2002;29:76–81.
 18. Tipre DN, Zoghbi SS, Liow JS, Green MV, Seidel J, Ichise M, et al. PET imaging of brain 5-HT_{1A} receptors in rat in vivo with [¹⁸F]FCWAY and improvement by successful inhibition of radioligand defluorination with miconazole. *J Nucl Med* 2006;47:345–53.
 19. Carson RE, Wu YJ, Lang LX, Ma Y, Der MG, Herscovitch P, et al. Brain uptake of the acid metabolites of ¹⁸F-labeled WAY 100635 analogs. *J Cereb Blood Flow Metab* 2003;23:249–60.
 20. Cliffe IA. Piperazine derivatives. EP 481744 A1, 1991.
 21. Campiani G, Butini S, Trotta F, Fattorusso C, Catalanotti B, Aiello F, et al. Synthesis and pharmacological evaluation of potent and highly selective D₃ receptor ligands: inhibition of cocaine-seeking behavior and the role of dopamine D₃/D₂ receptors. *J Med Chem* 2003;46:3822–39.
 22. Zhuang Z-P, Kung M-P, Mu M, Kung HF. Isoindol-1-one analogues of 4-(2'-methoxyphenyl)-1-[2'-[N-(2"-pyridyl)-p-iodobenzamido]ethyl]piperazine (*p*-MPPI) as 5-HT_{1A} receptor ligands. *J Med Chem* 1998;41:157–66.
 23. Zoghbi SS, Baldwin RM, Seibyl J, Charney DS, Innis RB. A radiotracer technique for determining apparent pK_a of receptor binding ligands. *J Label Compd Radiopharm* 1997;42:S136–8.
 24. Clark JD, Baldwin RL, Bayne KA, Brown MJ, Gebhart GF, Gunder JC, et al. Guide for the care and use of laboratory animals. Washington, DC: National Academy Press, 1996.
 25. Gandelman M, Baldwin RM, Zoghbi SS, Zea-Ponce Y, Innis RB. Evaluation of ultrafiltration for the free fraction determination of SPECT radiotracers: β-CIT, IBF and iomazenil. *J Pharm Sci* 1994;83L:1014–9.
 26. Shepherd RG. Process for the preparation of *o*-aryl-γ-butyrolactones. WO 94/12487. 1994.
 27. Shuomingshu FZSG. Preparation of the known neurotransmitter antagonist 1-[4-[4-(methoxyphenyl)-1-piperazinyl]-4-phenylbutyl]hexahydro-*1H*-azepine and its salts and enantiomers. CN 10766446. 1993.
 28. Ashwell MA. Amide derivatives. WO 9408983.1994.
 29. Lahti RA, Roberts RC, Cochrane EV, Primus RJ, Gallagher DW, Conley RR, et al. Direct determination of dopamine D₄ receptors in normal and schizophrenic brain tissue: a [³H]NGD-94-1 study. *Mol Psychiatry* 1998;3:528–33.
 30. Scheperjans F, Palomero-Gallagher N, Grefkes C, Scheicher A, Zilles K. Transmitter receptors reveal segregation of cortical areas in the human superior parietal cortex :relations to visual and somatosensory regions. *NeuroImage* 2005;28:362–79.
 31. Quick M, Police S, He I, Di Monte DA, Langston JW. Expression of D(3) receptor messenger RNA and binding sites in monkey striatum and substantia nigra after nigrostriatal degeneration: effect of levodopa treatment. *Neurosci* 2000;98:263–73.
 32. Varnäs K, Halldin C, Hall H. Autoradiographic distribution of serotonin transporters and receptor subtypes in human brain. *Human Brain Mapping* 2004;22:246–60.
 33. Burnet PW, Eastwood SL, Harrison PJ. [³H]WAY-100635 for 5-HT_{1A} receptor autoradiography in human brain; a comparison with [³H]8-OH-DPAT and demonstration of increased binding in the frontal cortex in schizophrenia. *Neurochem Int* 1997;30:565–74.
 34. Pike VW. Positron-emitting radioligands for studies in vivo—probes for human psychopharmacology. *J Psychopharmacol* 1993;7:139–58.
 35. Waterhouse RN. Determination of lipophilicity and its use as a predictor of blood-brain barrier penetration of molecular imaging agents. *Mol Imaging Biol* 2003;5:376–89.
 36. Farde L, Ginovart N, Itoh H, Lundkvist C, Pike VW, McCarron JA, et al. PET characterization of [*carbonyl*-¹¹C]WAY-100635 binding to 5-HT_{1A} receptors in the primate brain. *Psychopharmacology* 1997;133:196–202.
 37. Shetty HU, Zoghbi SS, McCarron JA, Liow J-S, Hong J, Pike VW. Characterization of in vivo rat metabolites of [*O-methyl*-¹¹C]RWAY by LC-MS. *J Label Compd Radiopharm* 2005;48:S278.
 38. Yasuno F, Zoghbi SS, McCarron JA, Ichise M, Gladding RL, Brown AK, et al. Quantification of serotonin 5-HT_{1A} receptors in monkey brain with [¹¹C](–)RWAY. *Synapse* 2006;60:510–20.